
**ORDER, DISORDER, AND PHASE TRANSITIONS
IN CONDENSED SYSTEMS**

Magnetic Resonance in Multilayer Gd/Si/Co Magnetic Films

**G. S. Patrin^{a,c}, V. O. Vas'kovskii^b, A. V. Svalov^b, E. V. Eremin^a,
M. A. Panova^a, and V. N. Vasil'ev^a**

^a*Kirenskiĭ Institute of Physics, Siberian Division, Russian Academy of Sciences,
Akademgorodok, Krasnoyarsk, 660036 Russia*

^b*Ural State University, pr. Lenina 51, Yekaterinburg, 620083 Russia*

^c*Krasnoyarsk State University, pr. Svobodnyĭ 79, Krasnoyarsk, 660041 Russia*

e-mail: patrin@iph.krasn.ru

Received July 22, 2005

Abstract—The magnetic properties of multilayer Gd/Si/Co magnetic films are experimentally studied by electron magnetic resonance and analyzed theoretically. The introduction of a semiconductor silicon interlayer is found to substantially affect the magnetic interlayer coupling and the magnetic dynamics of the system. The interlayer coupling is shown to be ferromagnetic for the $(\text{Gd/Si})_n$ films and to be antiferromagnetic for the $(\text{Gd/Si/Co/Si})_n$ films. The temperature dependences of the exchange parameters and the gyromagnetic ratios are determined. Possible mechanisms responsible for the formation of the interlayer coupling are discussed.

PACS numbers: 75.70.Cn, 76.50.+g

DOI: 10.1134/S1063776106010158

1. INTRODUCTION

$(\text{Gd/Si/Co/Si})_n$ films have been found to be very interesting objects for studying the modifications of interlayer exchange couplings in multilayer film structures under external actions. As was experimentally detected in [1], the temperature dependence of the magnetization of such films has a compensation point T_{comp} , whose value depends on the thickness of the silicon interlayer t_{Si} , just as in the case of bulk alloys rare-earth element–3d transition metal. In magnetic fields $H \leq 500$ Oe, a field-dependent specific feature is observed in the vicinity of this point at $T < T_{\text{comp}}$ [2]. The behavior of this specific feature can be explained on the assumption that, along with bilinear coupling, the interlayer coupling between magnetic layers contains a biquadratic contribution and that both contributions depend on the semiconductor-layer thickness, the temperature, and the magnetic field. In low magnetic fields, the magnetization of the films can behave similarly to spin-glass behavior [3], which also supports the presence of a biquadratic contribution in these films.

Obviously, the magnetic properties of this system depend not only on the states of the rare-earth and cobalt subsystems but also on their coupling. Therefore, we studied films in the row Gd/Si, Gd/Co, and Gd/Si/Co/Si to trace changes in the coupling between magnetic layers made of different metals depending on the interlayer material and thickness.

2. EXPERIMENTAL

The films to be studied were fabricated by ion-beam rf sputtering on a glass substrate [4]. The samples consisted of stacks and were protected from above and below by silicon of a thickness $t_{\text{Si}} = 200$ Å. The layer thicknesses in all films were the following: $t_{\text{Gd}} = 7.5$ nm, $t_{\text{Co}} = 3$ nm, and variable t_{Si} . All thickness parameters were set by the time of sputtering of the corresponding layers at the given deposition rates of different materials. With small-angle X-ray scattering, we detected a layered character of the films and confirmed the nominal values of the structure period (with an error of ± 2 Å). Moreover, as was shown by X-ray diffraction and electron-microscopic examination, the structure of the films is close to an amorphous structure. The magnetic structure of the Gd/Si/Co films was studied by electron magnetic resonance (EMR). The EMR parameters are sensitive to coupling factors that are responsible for the formation of a magnetic state. The measurements were performed in the microwave frequency range $\omega_{\text{MWF}} = 3.5$ –50.5 GHz in the range from liquid-nitrogen temperature to room temperature. The magnetic field lay in the film plane. The fact that the films have an amorphous structure was also supported by the absence of resonance-field anisotropy in the film plane.

3. $(\text{Gd/Si})_{40}$ FILMS

Figure 1 shows the experimental temperature dependences of the resonance field H_r (curve 1) and the microwave absorption intensity I (curve 4), which is

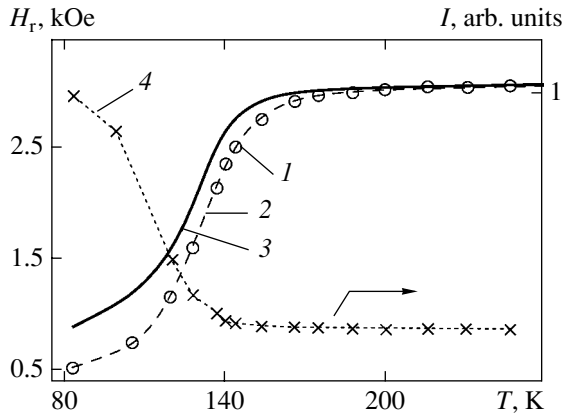


Fig. 1. Temperature dependences of (1) the resonance field (experiment) (2) calculation by Eq. (4), (3) calculation by Eq. (1) and (4) the magnetic-resonance line intensity of the $(\text{Gd/Si})_{40}$ film.

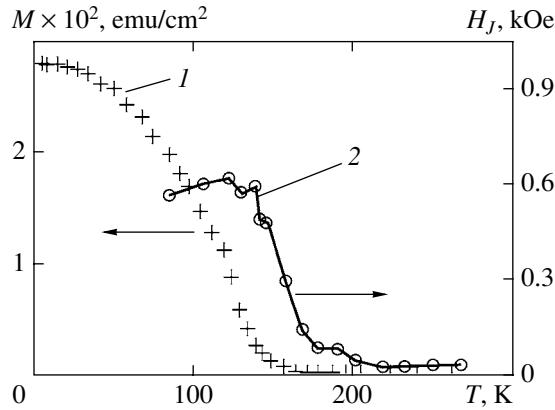


Fig. 2. Temperature dependences of (1) the magnetization of the $(\text{Gd/Si})_{40}$ film and (2) the exchange field of interlayer coupling.

determined as the area under the absorption curve, that are obtained for the $(\text{Gd/Si})_{40}$ sample with $t_{\text{Si}} = 2$ nm at a frequency $\omega_{\text{MWF}} = 9.3$ GHz. The spectrum is seen to consist of a single line with a near-Lorentzian shape. The temperature dependence of the magnetization (Fig. 2, curve 1) suggests that the entire film is ferromagnetic. Since the magnetic layers have an amorphous structure, their resonance properties can be considered by taking into account only the Zeeman energy and the energy related to a shape anisotropy. In this case, for the magnetic resonance frequency we have [5]

$$(\omega_1/\gamma)^2 = H_r(H_r + 4\pi m), \quad (1)$$

where

$$m = M/t \quad (2)$$

is the total magnetization of the whole film, $t = 40t_{\text{Gd}}$ is the total thickness of all magnetic layers, γ is the gyro-

magnetic ratio, H_r is the resonance field, and M is the magnetic moment of unit film surface (which is determined from Fig. 2, curve 1). The value of $\gamma_{\text{Gd}} = 3.05$ was calculated from the resonance field in the paramagnetic range. Calculation by this formula gives curve 3 in Fig. 1, which is seen to be inconsistent with experiment. Obviously, this discrepancy requires consideration of interlayer coupling. By making allowance for this finding, we can write the Hamiltonian of this system as

$$E_L = -\sum_{i<j} J_L \cos(\varphi_i - \varphi_j) - t_{\text{Gd}} \left[\left(\sum_i \mathbf{M}_i \right) \cdot \mathbf{H}_z + 4\pi \sum_i (M_i)_z^2 \right]. \quad (3)$$

Here, the first sum presents interlayer coupling; the second sum describes the Zeeman interaction, and the third sum is responsible for the demagnetization energy. The magnetic field H_z is assumed to lie in the film plane and to be directed along the z axis, J_L is the bilinear interlayer coupling constant, and the angles φ_i and φ_j specify the directions of the layer magnetizations and are measured from the direction of the applied magnetic field. If we take into account only nearest-layer coupling and combine the corresponding layers in a sublattice (the number of layers in the sublattice is 20), then the problem is reduced to a bilayer system [6] for which resonance frequencies are determined from Eq. (1) and the formula

$$(\omega_2/\gamma)^2 = H_r(H_r + H_M) + 2(2H_r + H_M)H_J + 4H_J^2, \quad (4)$$

where

$$H_M = 4\pi M, \quad H_J = J_L/(t_{\text{Gd}}M), \quad (5)$$

and M belong to the corresponding sublattice.

The processing of experimental dependence 1 in Fig. 1 with Eq. (4) shows that the interlayer “exchange” field H_J should have a temperature dependence given in Fig. 2, curve 2. In this case, the experimental and calculated results coincide with each other (cf. curves 1 and 2 in Fig. 1). As follows from the calculation, the interlayer coupling is ferromagnetic and the resulting coupling is caused by two processes. The first process consists in an increase in the number of coupling carriers in the semiconductor interlayer with the temperature (this increase strengthens the interlayer coupling), and the second process is a decrease in the magnetizations of the interacting subsystems (this decrease weakens the coupling energy). The exchange field H_J reflects the result of competition of these two mechanisms. The value of J_L estimated by Eq. (5) at the liquid-nitrogen temperature is about 10^{-4} erg/cm².

The temperature dependence of the microwave absorption line intensity has a shape that is similar to the temperature dependence of the magnetization of the whole film (cf. curve 4 in Fig. 1 and curve 1 in Fig. 2). Note that the microwave absorption intensity in this case is more than an order of magnitude weaker than that in the other films.

4. (Gd/Co)₂₀ FILMS

The (Gd/Co)₂₀ film having t_{Gd} and t_{Co} given above is known to undergo ferrimagnetic ordering with a magnetization compensation temperature $T_{\text{comp}} = 317$ K. In the microwave frequency range under study, the spectrum consists of a single line. Figure 3 shows the temperature dependences of H_r and I for this film at $\omega_{\text{MWF}} = 9.3$ GHz. The resonance field is seen to smoothly increase with the temperature, and the absorption line intensity decreases sharply by about an order of magnitude in the temperature range where a pure gadolinium film transforms into a paramagnetic state. In this temperature range, the temperature dependence of the magnetization of the (Gd/Co)₂₀ film exhibits no specific features (Fig. 7, curve 3). At a frequency $\omega_{\text{MWF}} = 19.8$ GHz, the ENR parameters behave similarly, although a signal is missed at a temperature $T \approx 200$ K (Fig. 3, inset). To find a high-frequency oscillation mode, we measured the field dependence of the frequency for the (Gd/Co)₂₀ film at $T = 139$ K (Fig. 4, curve 1); for comparison, we also give this dependence for a ball made of yttrium iron garnet (Fig. 4, curve 3). Nevertheless, we failed to detect a high-frequency mode. In the case where the exchange coupling between magnetic subsystems is much higher than the Zeeman energy, the field dependence of the frequency for the low-frequency mode of the film has a form typical of a two-sublattice platelike ferrimagnet [5]:

$$\omega/\gamma_{\text{eff}} = H + 4\pi(m_{\text{Gd}} - m_{\text{Co}}). \quad (6)$$

Here,

$$\gamma_{\text{eff}} = (m_{\text{Gd}} - m_{\text{Co}})/[(m_{\text{Gd}}/\gamma_{\text{Gd}}) - (m_{\text{Co}}/\gamma_{\text{Co}})]; \quad (7)$$

m_{Gd} and m_{Co} are the magnetizations of the gadolinium and cobalt subsystems, respectively, that are determined from Eq. (2); and γ_{Gd} and γ_{Co} are their gyromagnetic ratios. The mathematical processing of the experimental dependence (Fig. 4, curve 1) gives the following values for the quantities entering into Eq. (6): $m_{\text{Gd}} = 0.73$ G, $m_{\text{Co}} = 0.64$ G, $\gamma_{\text{Gd}} = 3.22$ GHz/kOe, and $\gamma_{\text{Co}} = 3.34$ GHz/kOe. The field dependence of the frequency calculated using these values is shown in Fig. 4, curve 2. The experimental and calculated data are seen to agree well with each other. The overshoot of the lowest point can be explained by the fact that the sample is in an unsaturated state at this frequency. As was shown in [2], the saturation field of this system at liquid-

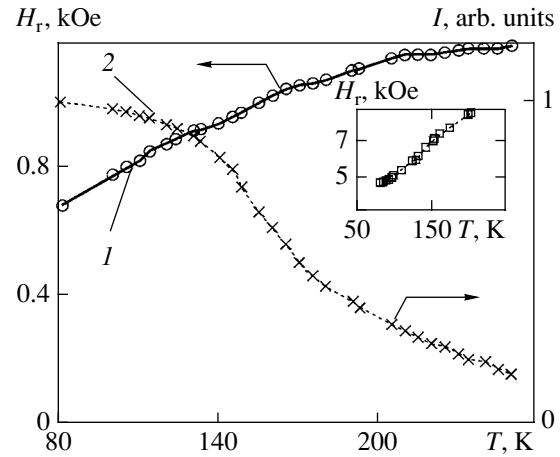


Fig. 3. Temperature dependences of (1) the resonance field and (2) the magnetic-resonance line intensity of the (Gd/Co)₂₀ film recorded at $\omega_{\text{MWF}} = 9.3$ GHz and (inset) $\omega_{\text{MWF}} = 19.8$ GHz.

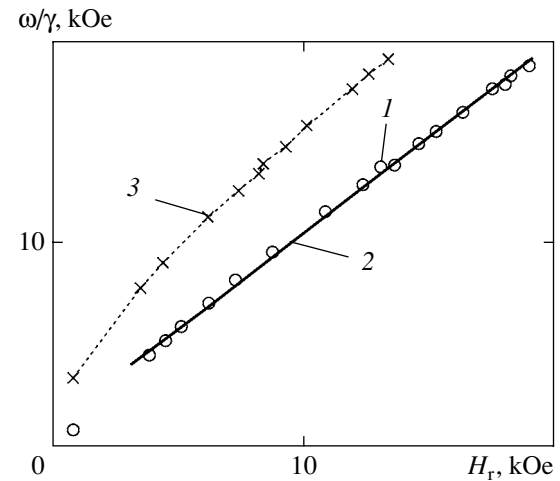


Fig. 4. Field dependence of the magnetic resonance frequency: (1) the (Gd/Co)₂₀ film, (2) calculation by Eq. (6), and (3) a ball of yttrium iron garnet. $T = 139$ K ($\gamma = 2.7$ GHz/kOe).

helium temperatures is about 500 Oe. If we compare the magnetizations of the gadolinium and cobalt subsystems obtained from the magnetic-resonance and magnetostatic measurements (Fig. 7, curve 3), the discrepancy does not exceed 5%.

5. (Gd/Si/Co/Si)₂₀ FILMS

In the presence of a silicon interlayer, the situation becomes much more complex. As was described in the Introduction, even small thicknesses of this interlayer substantially modify the interlayer couplings in the (Gd/Si/Co/Si)₂₀ films. In this case, the magnetic resonance spectrum consists of two superimposed Lorentzian lines. Figure 5 illustrates the variation of the spectrum for the film with $t_{\text{Si}} = 1.0$ nm at two microwave fre-

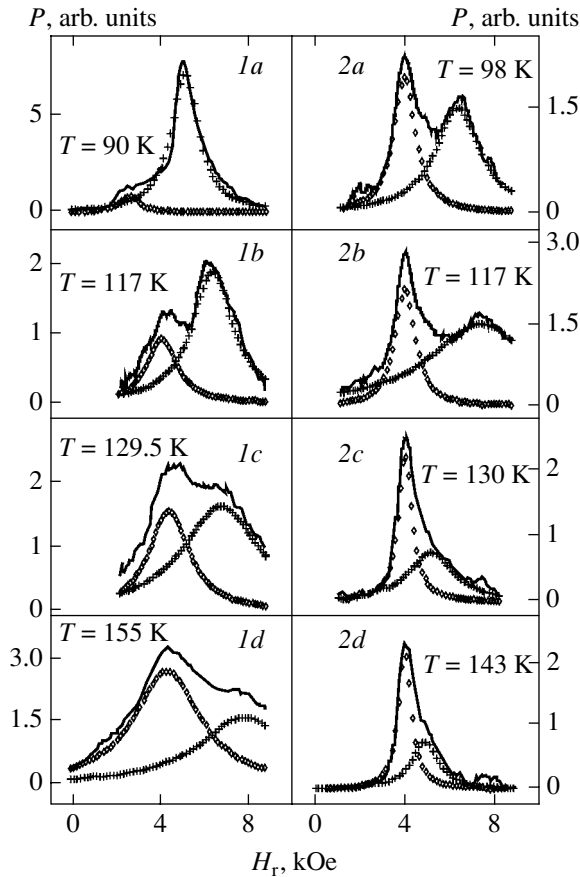


Fig. 5. Magnetic resonance spectrum for the $(\text{Gd}/\text{Si}/\text{Co}/\text{Si})_{20}$ film with $t_{\text{Si}} = 1.0$ nm: (1) $\omega_{\text{MWF}} = 9.3$ GHz and (2) $\omega_{\text{MWF}} = 24$ GHz.

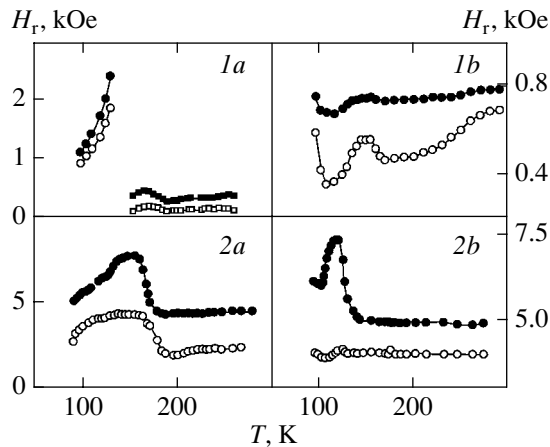


Fig. 6. Temperature dependences of the resonance field in the $(\text{Gd}/\text{Si}/\text{Co}/\text{Si})_{20}$ films: (1) $\omega_{\text{MWF}} = 9.3$ GHz and (2) $\omega_{\text{MWF}} = 24$ GHz. (a) $t_{\text{Si}} = 0.5$ nm and (b) $t_{\text{Si}} = 1.0$ nm.

quencies with the temperature. As the temperature increases, the intensity is seen to transfer from a high- to low-frequency mode. Figure 6 shows the temperature dependences of the resonance field for the films

with silicon interlayer thicknesses $t_{\text{Si}} = 0.5$ and 1.0 nm at microwave frequencies $\omega_{\text{MWF}} = 9.3$ and 24 GHz. Figure 7 (curves 1, 2) presents the magnetostatic results for these films obtained in a field $H = 1$ kOe. It is seen that the magnetic-resonance parameters have a specific feature in the vicinity of the compensation temperature, which is most pronounced in fields $H < 200$ Oe [2, 3]. Note that, in high magnetic fields, the effect of magnetization compensation in these films is smeared. For magnetic resonance in the case under study ($t_{\text{Si}} = 0.5$ and 1.0 nm), the temperature of the specific feature shifts toward low temperatures as the microwave frequency increases; this is evidenced by the behavior of the humps in the temperature dependence of the resonance field (Fig. 6, panels 1, 2). These data correlate with the results of [2], where the authors detected the effect of a silicon interlayer between magnetic layers on their interlayer coupling in low magnetic fields and a shift in the specific feature toward low temperatures.

The magnetic-resonance data obtained for the gadolinium–cobalt films with a silicon interlayer cannot be accounted for in terms of a simple model where the exchange field is taken to be much higher than the applied magnetic field. In our situation, these fields are comparable in the best case, and, in low magnetic fields ($H \leq 500$ Oe), the magnetic structure is likely to be canted rather than strictly antiparallel. In the absence of a magnetic anisotropy, such a structure can be realized due to biquadratic coupling caused by the introduction of a semiconductor silicon interlayer.

To describe the magnetic properties of these films, we have to add a term that takes into account the contribution of biquadratic coupling to Hamiltonian (3). As a result, we have

$$E = E_L - \sum_{i < j} J_Q \cos^2(\varphi_i - \varphi_j), \quad (8)$$

where E_L is set by Eq. (3), J_Q is the biquadratic coupling constant, and the other designations are traditional. When taking into account the coupling of only neighboring layers and when combining the layers of one ferromagnetic metal into a sublattice, we can reduce the problem to a trilayer system.

In this case, the magnetic resonance spectrum of a trilayer system with Hamiltonian of type (8) was calculated in [6], where a relation connecting the microwave frequency and the magnetic field was derived in the general form. We rewrite this relation in the form where J -containing terms are separated (Appendix, Eq. (A)) and consider the situation where a film is in its saturated state, i.e., in magnetic fields higher than the spin-flop field, and where the magnetization directions of the ferromagnetic subsystems coincide with the direction of the applied field. The experimental results corresponding to this approximation are given in Fig. 6, panel 2. The experimental data are fitted provided that the dependences of the magnetization and the resonance

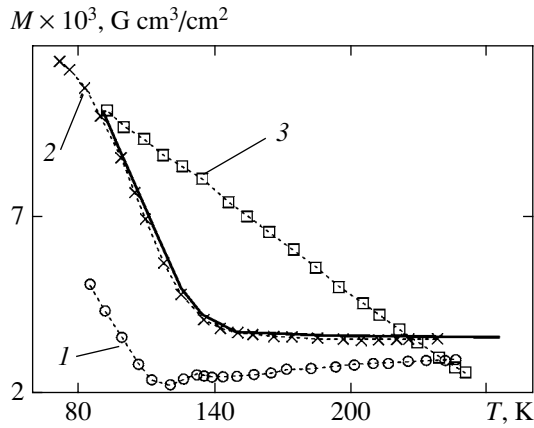


Fig. 7. Temperature dependences of the magnetization of the $(\text{Gd/Si/Co/Si})_{20}$ films recorded at $t_{\text{Si}} = (1)$ 0.5, (2) 1.0, and (3) 0 nm in a field $H = 1$ kOe. The solid line is calculation.

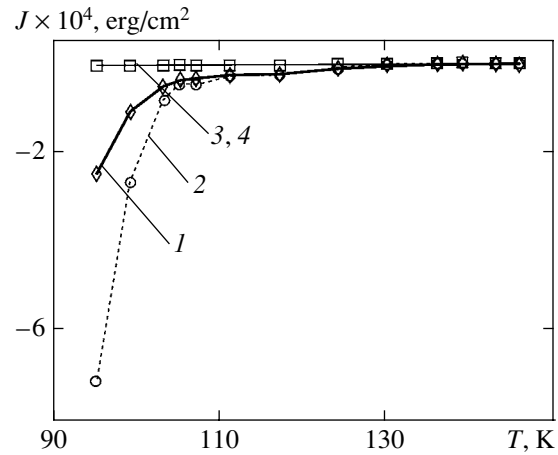


Fig. 8. Temperature dependences of the interlayer coupling constants in the $(\text{Gd/Si/Co/Si})_{20}$ films: (1, 3) J_1 at $t_{\text{Si}} = 0.5$ nm and (2, 4) J_2 at $t_{\text{Si}} = 1.0$ nm. $\omega_{\text{MWF}} = 24$ GHz.

fields are taken from experiment. Moreover, we used curve 2 in Fig 7, since the saturation magnetizations of both compounds in the multilayer films are the same (their saturation fields are different) [2]. As fitting parameters we used γ_{Gd} and γ_{Co} . The structure of expression (A) is such that exchange constants enter in it in the combination $J = J_L + 2J_Q$, and it is impossible to separate bilinear and biquadratic contributions. To separate these contributions, it is necessary to use the fact that, in an unsaturated state, they have different dependences on the angles between the applied magnetic field and the directions of the ferromagnetic systems. Therefore, to extract J_L and J_Q dependences from experimental data in order to determine the equilibrium angles of the subsystem magnetizations, we should record the temperature dependences of these magnetizations in an unsaturated state in magnetic fields over the entire range of resonance fields, which seems to be unreasonable.

Figure 8 shows the calculated temperature dependences of J_1 (curves 1, 3) and J_2 (curves 2, 4) for the films with $t_{\text{Si}} = 0.5$ and 1.0 nm, respectively. Fitting is optimum at the following gyromagnetic ratios: $\gamma_{1\text{Gd}} = 2.52$ GHz/kOe, $\gamma_{1\text{Co}} = 1.26$ GHz/kOe, $\gamma_{2\text{Gd}} = 2.255$ GHz/kOe, and $\gamma_{2\text{Co}} = 1.205$ GHz/kOe (the subscripts correspond to panels 1 and 2 in Fig. 6). As would be expected, the interlayer exchange is negative. In the case of negative exchange and the state of magnetic saturation, Layadi [6] theoretically showed that one oscillation mode (optical mode) depends on the interlayer coupling and the other mode (acoustic mode) is independent of the interlayer coupling. It is this behavior that is illustrated in Fig. 8. Curves 1 and 2 were obtained by processing the dependences of high-frequency modes in Fig. 6, panel 2, and curves 3 and 4 were obtained by processing low-frequency modes. It is also seen from Fig. 8 that the interlayer coupling con-

stant increases in absolute value with the silicon interlayer thickness. This tendency agrees with earlier results; e.g., with the results obtained for $(\text{Fe/Si})_n$ films [7, 8], where the interlayer coupling was found to be maximum at $t_{\text{Si}} \approx 2.0$ nm. In this case, just as in the case of the $(\text{Gd/Si})_n$ film, the interlayer coupling results from two processes: an increase in the charge carrier concentration in the semiconductor with the temperature and a decrease in the magnetization of the gadolinium subsystem. However, as the temperature decreases, one should expect a limited increase in the coupling because of conduction-electron freezing-out in the interlayer. Although conduction can occur via band tails due to the amorphous structure of the semiconductor, it is weak, as was shown for Fe/Si/Fe films [9].

6. CONCLUSIONS

The parameters of interlayer coupling between ferromagnetic layers in films with a semiconductor silicon interlayer have been established to be temperature-independent. The effect of the silicon interlayer is most pronounced in gadolinium-cobalt films. In this case, the gyromagnetic ratios differ substantially from the values obtained for magnetic resonance in other systems. This finding indicates that the semiconductor interlayer changes the electron density inside the ferromagnetic layers, which manifests itself in the formation of the magnetic moments of magnetic ions. However, these phenomena should be studied by magnetoresistive methods.

ACKNOWLEDGMENTS

This work was supported by the Russian Foundation for Basic Research (project nos. 05-02-16676-a,

04-02-16485-a) and the federal program “Russian Universities” (grant no. 01.01.097).

APPENDIX

For the case of $\varphi_H = \varphi_1 = \varphi_2 = 0$, the magnetic resonance spectrum of a trilayer film is calculated by the formula

$$\begin{aligned}
 & J^2 \left\{ (m_1 + m_2)H[m_1(H + 4\pi M_1) \right. \\
 & \left. + m_2(H + 4\pi M_2)] - \left(\frac{m_1}{\gamma_1} + \frac{m_2}{\gamma_2} \right)^2 \omega^2 \right\} \\
 & + J \left\{ m_1 m_2 H^2 [m_1(H + 4\pi M_1) + m_2(H + 4\pi M_2)] \right. \\
 & \left. + (m_1 + m_2)m_1 m_2 H(H + 4\pi M_1)(H + 4\pi M_2) \right. \\
 & \left. - m_1 m_2 \left[m_1 \left(\frac{H}{\gamma_2^2} + \frac{H + 4\pi M_2}{\gamma_1^2} \right) \right. \right. \quad (A) \\
 & \left. \left. + m_2 \left(\frac{H}{\gamma_1^2} + \frac{H + 4\pi M_1}{\gamma_2^2} \right) \right] \omega^2 \right\} \\
 & + \left(\frac{m_1 m_2}{\gamma_1 \gamma_2} \right)^2 \omega^4 - (m_1 m_2)^2
 \end{aligned}$$

$$\times \left[\frac{H(H + 4\pi M_1)}{\gamma_2^2} + \frac{H(H + 4\pi M_2)}{\gamma_1^2} \right] \omega^2$$

$$- (m_1 m_2)^2 H^2 (H + 4\pi M_1)(H + 4\pi M_2) = 0.$$

Here, M_i is the magnetization of the i th subsystem; $m_i = t_i M_i$; t_i is the total thickness of each ferromagnet; $i = 1, 2$ stands for Gd and Co, respectively; $\gamma_1 = \gamma_{\text{Gd}}$; and $\gamma_2 = \gamma_{\text{Co}}$.

REFERENCES

1. L. N. Merenkov, A. B. Chizhik, S. L. Gnatchenko, *et al.*, *Fiz. Nizk. Temp.* **27**, 188 (2001) [*Low Temp. Phys.* **27**, 137 (2001)].
2. G. S. Patrin, V. O. Vas'kovskii, D. A. Velikanov, and A. V. Svalov, *Pis'ma Zh. Éksp. Teor. Fiz.* **75**, 168 (2002) [*JETP Lett.* **75**, 159 (2002)].
3. G. S. Patrin, V. O. Vas'kovskii, D. A. Velikanov, *et al.*, *Phys. Lett. A* **309**, 155 (2003).
4. V. O. Vas'kovskii, D. Garsia, A. V. Svalov, *et al.*, *Fiz. Met. Metalloved.* **86**, 48 (1988).
5. A. G. Gurevich, *Magnetic Resonance in Ferrites and Antiferromagnets* (Nauka, Moscow, 1973) [in Russian].
6. A. Layadi, *Phys. Rev. B* **65**, 104422 (2002).
7. S. Toscano, B. Briner, H. Hopster, and M. Landolt, *J. Magn. Magn. Mater.* **114**, L6 (1992).
8. G. S. Patrin, N. V. Volkov, and V. P. Kononov, *Pis'ma Zh. Éksp. Teor. Fiz.* **68**, 287 (1998) [*JETP Lett.* **68**, 307 (1998)].
9. G. S. Patrin, S. G. Ovchinnikov, D. A. Velikanov, and V. P. Kononov, *Fiz. Tverd. Tela (St. Petersburg)* **43**, 1643 (2001) [*Phys. Solid State* **43**, 1712 (2001)].

Translated by K. Shakhlevich